



# Effect of air composition ( $\text{N}_2$ , $\text{O}_2$ , Ar, and $\text{H}_2\text{O}$ ) on $\text{CO}_2$ and $\text{CH}_4$ measurement by wavelength-scanned cavity ring-down spectroscopy: calibration and measurement strategy

H. Nara<sup>1</sup>, H. Tanimoto<sup>1</sup>, Y. Tohjima<sup>1</sup>, H. Mukai<sup>1</sup>, Y. Nojiri<sup>1</sup>, K. Katsumata<sup>1</sup>, and C. W. Rella<sup>2</sup>

<sup>1</sup>National Institute for Environmental Studies, 16-2 Onogawa, Tsukuba, Ibaraki, 305-8506, Japan

<sup>2</sup>Picarro Inc., 3105 Patrick Henry Drive, California, Santa Clara, 94054, USA

Correspondence to: H. Nara (nara.hideki@nies.go.jp)

Received: 22 June 2012 – Published in Atmos. Meas. Tech. Discuss.: 20 July 2012

Revised: 8 October 2012 – Accepted: 18 October 2012 – Published: 12 November 2012

**Abstract.** We examined potential interferences from water vapor and atmospheric background gases ( $\text{N}_2$ ,  $\text{O}_2$ , and Ar), and biases by isotopologues of target species, on accurate measurement of atmospheric  $\text{CO}_2$  and  $\text{CH}_4$  by means of wavelength-scanned cavity ring-down spectroscopy (WS-CRDS). Changes of the background gas mole fractions in the sample air substantially impacted the  $\text{CO}_2$  and  $\text{CH}_4$  measurements: variation of  $\text{CO}_2$  and  $\text{CH}_4$  due to relative increase of each background gas increased as  $\text{Ar} < \text{O}_2 < \text{N}_2$ , suggesting similar relation for the pressure-broadening effects (PBEs) among the background gas. The pressure-broadening coefficients due to variations in  $\text{O}_2$  and Ar for  $\text{CO}_2$  and  $\text{CH}_4$  are empirically determined from these experimental results. Calculated PBEs using the pressure-broadening coefficients are linearly correlated with the differences between the mole fractions of  $\text{O}_2$  and Ar and their ambient abundances. Although the PBEs calculation showed that impact of natural variation of  $\text{O}_2$  is negligible on the  $\text{CO}_2$  and  $\text{CH}_4$  measurements, significant bias was inferred for the measurement of synthetic standard gases. For gas standards balanced with purified air, the PBEs were estimated to be marginal (up to 0.05 ppm for  $\text{CO}_2$  and 0.01 ppb for  $\text{CH}_4$ ) although the PBEs were substantial (up to 0.87 ppm for  $\text{CO}_2$  and 1.4 ppb for  $\text{CH}_4$ ) for standards balanced with synthetic air. For isotopic biases on  $\text{CO}_2$  measurements, we compared experimental results and theoretical calculations, which showed excellent agreement within their uncertainty. We derived instrument-specific water correction functions empirically for three WS-CRDS instruments (Picarro EnviroSense 3000i, G-1301, and G-2301), and evaluated the transferability of

the water correction function from G-1301 among these instruments. Although the transferability was not proven, no significant difference was found in the water vapor correction function for the investigated WS-CRDS instruments as well as the instruments reported in the past studies within the typical analytical precision at sufficiently low water concentrations ( $< 0.7\%$  for  $\text{CO}_2$  and  $< 0.6\%$  for  $\text{CH}_4$ ). For accurate measurements of  $\text{CO}_2$  and  $\text{CH}_4$  in ambient air, we concluded that WS-CRDS measurements should be performed under complete dehumidification of air samples, or moderate dehumidification followed by application of a water vapor correction function, along with calibration by natural air-based standard gases or purified air-balanced synthetic standard gases with the isotopic correction.

## 1 Introduction

Since atmospheric carbon dioxide ( $\text{CO}_2$ ) is one of the most important trace gases in controlling the Earth's climate (e.g. surface temperature), much attention has been paid to the understanding of the global distribution of  $\text{CO}_2$  during the last 50 yr of the twentieth century. Recent studies have pointed out that better understanding of non- $\text{CO}_2$  greenhouse gases (GHGs) such as methane ( $\text{CH}_4$ ) is also needed to mitigate future climate change more effectively (Aydin et al., 2011; Kai et al., 2011; Montzka et al., 2011). Towards better and inclusive estimates of GHG emissions from terrestrial sources, top-down estimates by means of inverse model calculations are a key approach to decrease the uncertainty

of bottom-up estimates, which are largely based on emission inventories. Ambient greenhouse gas observations have been extensively performed by a number of researchers using aircraft, ships, and ground-based stations (e.g. Keeling, 1960; Lowe et al., 1979; Conway et al., 1994; Dlugokencky et al., 1995; Keeling et al., 1995; Matsueda and Inoue, 1996; Prinn et al., 2000; Cunnold et al., 2002; Brenninkmeijer et al., 2007; Machida et al., 2008; Rigby et al., 2008; Terao et al., 2011). Although these observations have revealed detailed distributions of GHGs, ambient monitoring data are still sparse and less reliable in developing countries where GHG emissions are increasing rapidly due to increasing socioeconomic activities (Marquis and Tans, 2008). These studies point to the need for a comprehensive worldwide GHG observational system.

Ground- and satellite-based spectroscopic observation of GHGs is a powerful method to capture global distributions of GHGs. For example, the Total Carbon Column Observing Network (TCCON), a network of ground-based solar absorption Fourier transform infrared spectrometers, provides measurements of the total column abundances of CO<sub>2</sub>, CH<sub>4</sub>, N<sub>2</sub>O, HF, CO, H<sub>2</sub>O, and HDO at 18 sites (Wunch et al., 2012). Atmospheric Infrared Sounder (AIRS, which is mounted on the Aqua satellite) and the Scanning Imaging Absorption Spectrometer for Atmospheric Chartography (SCIAMACHY, which is mounted on the ENVISAT satellite; SCIAMACHY stopped its operation in May 2012 due to sudden communication blackout) provide global images of total column abundance of CO<sub>2</sub> and CH<sub>4</sub> (Buchwitz et al., 2005; Xiong et al., 2010). Analysis of CO<sub>2</sub> and CH<sub>4</sub> data obtained with the Greenhouse Gas Observing Satellite (GOSAT), launched on 23 January 2009, has begun recently (Saitoh et al., 2009; Yokota et al., 2009; Yoshida et al., 2011). However, these satellite observations need to be supported by in-situ observations for validation and calibration of GHG concentrations retrieved from observation data.

During the last several decades, non-dispersive infrared (NDIR) spectroscopy and gas chromatography (GC) have been widely used as a routine method to observe CO<sub>2</sub> and CH<sub>4</sub> in ambient air (e.g., Conway et al., 1994; Dlugokencky et al., 1995) due to their high accuracy and precision. Optical techniques including tunable diode laser absorption spectroscopy (TDLAS) (Webster et al., 1994; Richard et al., 2002), quantum cascade laser spectroscopy (QCL) (Webster et al., 2001), and Fourier transform infrared spectroscopy (FTIR) (Esler et al., 2000; Grutter, 2003) have also been used to measure CO<sub>2</sub> and CH<sub>4</sub> in the atmosphere. In parallel with these techniques, other laser-based measurements have been developed based on cavity ring-down spectroscopy (CRDS) (O'Keefe and Deacon, 1988), integrated cavity-output spectroscopy (ICOS) (O'Keefe, 1998), off-axis integrated cavity-output spectroscopy (OA-ICOS) (O'Keefe et al., 1999; Paul et al., 2001; Baer et al., 2002), and cavity enhanced absorption spectroscopy (CEAS) (Berden et al., 1999). More recently, advancements in the optical

measurement technology greatly contributed to the improved performance of these optical measurement techniques, including closed path FTIR (Griffith et al., 2012; Hammer et al., 2012), and to the development of new measurement techniques such as wavelength-scanned cavity ring-down spectroscopy (WS-CRDS) (Crosson, 2008). These techniques have achieved accuracy and precision for atmospheric CO<sub>2</sub> and CH<sub>4</sub> measurement, which are comparable or better than those of conventional NDIR and GC techniques.

The WS-CRDS manufactured by Picarro, Inc. (Santa Clara, CA, USA) successfully fulfils increasing demands for scientists to expand routine monitoring at remote sites because the instrument is compact, lightweight, and easily maintained, resulting in excellent long-term stability with high precision and time resolution. For example, Chen et al. (2010) conducted airborne observations of CO<sub>2</sub> and CH<sub>4</sub> over the Amazon rain forest using a WS-CRDS instrument during the Balanço Atmosférico Regional de Carbono na Amazônia campaign in 2009. Beginning in April 2009, Winderlich et al. (2010) used the WS-CRDS instrument for continuous observations of CO<sub>2</sub> and CH<sub>4</sub> at a tall tower observation site (Zotino Tall Tower Observatory, established by Kozlova and Manning, 2009) in central Siberia. Messerschmidt et al. (2011) used the WS-CRDS instrument in aircraft observational campaigns over European sites of The Total Carbon Column Observing Network to calibrate measurements of CO<sub>2</sub> and CH<sub>4</sub> column abundances obtained by satellite observations. Richardson et al. (2012) deployed WS-CRDS instruments at five tall tower stations. These investigators tested long-term stability of the WS-CRDS instruments under the field environments, and showed excellent stability of the WS-CRDS instruments with CO<sub>2</sub> drift being less than 0.38 ppm for 30 months.

Chen et al. (2010) examined the analytical performance of a Picarro WS-CRDS instrument in detail. They revealed that CO<sub>2</sub> and CH<sub>4</sub> measurements were affected by changes in the concentration of water vapor, background gases, and isotopologues of the target gas. For example, these investigators examined empirical relationships between magnitude of water interference, consisting of the dilution and line-broadening effects, and the water vapor concentrations measured by WS-CRDS, showing substantial interference (approximately 2.5 and 2.1 % decrease for CO<sub>2</sub> and CH<sub>4</sub>, respectively, at 2 % water vapor concentration). Based on the experimental results, these investigators derived the water correction function and assessed its transferability between the WS-CRDS instruments, model G-1301 and G-1301-m. They suggested that a single water vapor correction function can be applied universally to a given model of WS-CRDS instrument if calibrated to the same scale of water vapor. Chen et al. (2010) made a comparison of CO<sub>2</sub> measurements between WS-CRDS and NDIR during the flight observation campaign for validation of the WS-CRDS measurements. These investigators revealed that CO<sub>2</sub> measurements of the WS-CRDS were biased from those of NDIR due to the

difference in the mole fraction of CO<sub>2</sub> minor isotopologues and the difference of line-broadening and -narrowing effects on the CO<sub>2</sub> absorption spectrum between the sample air and the synthetic standard gas. They examined the impact of the line-broadening and -narrowing effects as well as the isotopic difference, which were estimated to be up to 1.68 ppm, and typically 0.14 ~ 0.16 ppm, respectively. After correcting these biases, good agreement was obtained between the two methods (within 0.05 ~ 0.09 ppm). Chen et al. (2010) recommended the use of ambient air-based standard gas for WS-CRDS calibration to avoid these biases while the impact of such variations on the CO<sub>2</sub> and CH<sub>4</sub> measurements has not been tested experimentally.

The World Meteorological Organization recommends interlaboratory compatibilities of better than 0.1 ppm for CO<sub>2</sub> and 2 ppb for CH<sub>4</sub> (WMO, 2009), where high accuracy measurements is required for CO<sub>2</sub> and CH<sub>4</sub> measurements. To achieve the high accuracy measurements using the WS-CRDS instrument, the factors affecting WS-CRDS measurements should be understood in detail and corrected if needed before data are shared by the community for further investigation. In this study, we investigated (1) the correlations between the pressure-broadening effects (PBEs) and variations in background gases N<sub>2</sub>, O<sub>2</sub>, and Ar; (2) the correction for the isotopic bias on the CO<sub>2</sub> measurements through comparison between experimental results and theoretical calculations; and (3) the transferability of empirically determined water correction function among different three WS-CRDS models and differences in the water correction values from these functions as well as from past studies.

## 2 Wavelength-scanned cavity ring-down spectroscopy

In this study, we utilized three models of WS-CRDS instruments, the EnviroSense 3000i, G-1301, and G-2301, which are available from Picarro, Inc. (Santa Clara, CA, USA). Because detailed principles and the fundamental performance of the WS-CRDS instruments have been described elsewhere (Crosson, 2008), only a brief explanation is given here. The WS-CRDS can measure CO<sub>2</sub>, CH<sub>4</sub>, and H<sub>2</sub>O simultaneously, operating on the principle of laser absorption spectroscopy. The WS-CRDS instrument consists of a laser source, a high-precision wavelength monitor, a high-finesse optical cavity, a photodetector, and a data processing computer. An air sample is supplied into the optical cavity using a diaphragm pump while the pressure of the optical cavity is kept constant. A laser light at a specific wavelength from the light source is emitted into the optical cavity, and then the laser is shut off when the measurement signals from the photodetector achieve a steady-state condition. The optical cavity is equipped with three high-reflectivity mirrors (< 99.995 %) and has a volume of 40 ml (for the EnviroSense 3000i, the cavity volume is 35 ml). The cavity pressure and temperature are controlled rigorously at 140.00 ± 0.05 Torr

and 40.00 ± 0.01 °C, respectively. The laser light confined in the cavity circulates among the three mirrors, resulting in an effective optical path length of about 20 km. The light intensity decays in time as the light leaks through the mirrors and is absorbed by target molecules while the difference in the decay (ring-down) time with and without laser absorption by the target molecule is proportional to the mole fraction of the target molecule in a sample gas. Based on the difference in the ring-down time, the mole fractions of the target gases are quantified, irrespective of the initial intensity of the laser light. In order to achieve high precision and sensitivity, the WS-CRDS scanned the intensity of the leaking light over the target gas absorption line using the high-precision wavelength monitor with a wavelength resolution of 0.0003 cm<sup>-1</sup>: 1603 nm for <sup>12</sup>C<sup>16</sup>O<sub>2</sub> and 1651 nm for <sup>12</sup>CH<sub>4</sub> and H<sub>2</sub><sup>16</sup>O in real time using the photodetector during each measurement cycle, allowing to model the absorption peak-shape of the target gas from up to 10 points with a Galatry function (Galatry, 1961). Based on the absorption peak maximum of the modeled absorption line-shape, the WS-CRDS calculates mole fraction of target gas. The typical analytical precision of CO<sub>2</sub> and CH<sub>4</sub> measurements for 5 min obtained by the WS-CRDS instruments used in this study were very similar: 0.04 ppm and 0.3 ppb for EnviroSense 3000i, 0.05 ppm and 0.3 ppb for G-1301, 0.03 ppm and 0.3 ppb for G-2301, respectively.

## 3 Pressure-broadening effects of background gases

Past studies revealed that infrared spectroscopic analysis of CO<sub>2</sub> using NDIR is biased depending on the different types of NDIR instrument by change of temperature, pressure, and matrix gas composition (Bischof, 1975; Pearman and Garratt, 1975; Griffith, 1982; Griffith et al., 1982). This bias results from absorption line broadening and narrowing of CO<sub>2</sub> molecules due to random thermal motion, and collisions. Random thermal motion and intermolecular collisions produce line-broadening effects (referred to as Doppler and Lorentzian broadening effects, respectively), while the velocity-changing collisions produce line-narrowing effects (a kind of Dicke narrowing), which diminish the Doppler broadening effects (Dicke, 1953; Varghese and Hanson, 1984).

The WS-CRDS models the absorption line-shape of the target gases using the Galatry function, which describes the above-mentioned line-broadening and -narrowing effects simultaneously (Galatry, 1961). In the Galatry function, the Doppler and Lorentzian broadening effects and the line-narrowing effects are parameterized as the variables  $x$ ,  $y$ , and  $z$ , respectively, and the function is represented by these three variable parameters (Varghese and Hanson, 1984). For WS-CRDS measurements, the Galatry line-shape is determined by the line-width parameters  $y$  and  $z$  because the Doppler broadening effect ( $x$ ), when expressed as a function

of temperature, can be considered a constant value in a well-controlled optical cavity. In contrast, the magnitudes of Lorentzian broadening ( $y$ ) and the line-narrowing effect ( $z$ ) of the target gas depend on matrix gas composition. Thus the line-shape of the target gas is affected only by the matrix gas composition in the WS-CRDS measurements. Because the line-narrowing effect is of much smaller magnitude than Lorentzian broadening effect, we hereafter refer to both effects collectively as pressure-broadening effects (PBEs).

If we assume that PBEs are linearly proportional to infinitesimal changes in the matrix gas composition, we can approximate the magnitude of PBEs on CO<sub>2</sub> and CH<sub>4</sub> absorption spectral lines. For multicomponent gas mixtures, line-width parameters  $y$  and  $z$  for the specific spectral absorption lines of the target gases in the mixture are given by the sum of the pure gas line-width parameters weighted by each gas's mole fraction in the mixture. For atmospheric observation, the line-width parameters  $y$  and  $z$  depend on the composition of the background gases (N<sub>2</sub>, O<sub>2</sub>, and Ar), and thus the effective line parameters  $y_{\text{eff}}$  and  $z_{\text{eff}}$  are expressed as follows:

$$\begin{aligned} y_{\text{eff}} &= c_{\text{N}_2} y_{\text{N}_2} + c_{\text{O}_2} y_{\text{O}_2} + c_{\text{Ar}} y_{\text{Ar}} \\ z_{\text{eff}} &= c_{\text{N}_2} z_{\text{N}_2} + c_{\text{O}_2} z_{\text{O}_2} + c_{\text{Ar}} z_{\text{Ar}}, \end{aligned} \quad (1)$$

where  $c$  is the mole fraction for the background gas indicated as subscript. The variations of the background gases in the atmosphere are usually small enough to approximate the Galatry function by a two-dimensional Taylor expansion about  $y_{\text{eff}}$  and  $z_{\text{eff}}$  given for nominal atmospheric composition:

$$\begin{aligned} G(y + \Delta y_{\text{eff}} z + \Delta z_{\text{eff}}) &= G(y, z) + \frac{\partial}{\partial y} G(y, z) \Delta y_{\text{eff}} \\ &+ \frac{\partial}{\partial z} G(y, z) \Delta z_{\text{eff}}. \end{aligned} \quad (2)$$

$G$  expresses the maximum value of the line-shape function defined by the Galatry function with line-width parameters  $y$  and  $z$  at measured wavelength (1603 nm for CO<sub>2</sub>, 1651 nm for CH<sub>4</sub>), and  $\Delta y_{\text{eff}}$  and  $\Delta z_{\text{eff}}$  are defined by Eq. (1) corresponding to infinitesimal changes of the background gases. Equation (2) is then rearranged to

$$\frac{G(y + \Delta y_{\text{eff}}, z + \Delta z_{\text{eff}}) - G(y, z)}{G(y, z)} = k_y \Delta y_{\text{eff}} + k_z \Delta z_{\text{eff}}, \quad (3)$$

where

$$k_y = \frac{1}{G(y, z)} \frac{\partial}{\partial y} G(y, z) \quad k_z = \frac{1}{G(y, z)} \frac{\partial}{\partial z} G(y, z). \quad (4)$$

From Eqs. (1) and (3), we obtain the following equation:

$$\text{PBE} = \frac{G(y + \Delta y_{\text{eff}}, z + \Delta z_{\text{eff}}) - G(y, z)}{G(y, z)} \times c_{\text{target}} \quad (5)$$

$$\begin{aligned} &= c_{\text{target}} \{ (k_y y_{\text{N}_2} + k_z z_{\text{N}_2}) \delta c_{\text{N}_2} + (k_y y_{\text{O}_2} + k_z z_{\text{O}_2}) \delta c_{\text{O}_2} \\ &+ (k_y y_{\text{Ar}} + k_z z_{\text{Ar}}) \delta c_{\text{Ar}} \}, \end{aligned} \quad (6)$$

where PBE indicates the magnitude of PBEs on the target gas (units corresponding to that of the target gas);  $c_{\text{target}}$  is the mole fraction of the target gas;  $\delta c$  indicates variation of the inert gas indicated as subscript from its nominal composition. Unit for the variable,  $c_{\text{target}}$  and  $\delta c$  is given in ppm for CO<sub>2</sub> and in ppb for CH<sub>4</sub>. Here we define a dimensionless pressure-broadening coefficient  $\varepsilon$  per target gas mole fraction to express  $(k_y y_i + k_z z_i)$ . We then rearrange Eq. (5) using  $\varepsilon$ :

$$\text{PBE}/c_{\text{target}} = \varepsilon_{\text{N}_2} \delta c_{\text{N}_2} + \varepsilon_{\text{O}_2} \delta c_{\text{O}_2} + \varepsilon_{\text{Ar}} \delta c_{\text{Ar}}. \quad (7)$$

Among each inert gas, following approximation holds as:

$$\delta c_{\text{N}_2} + \delta c_{\text{O}_2} + \delta c_{\text{Ar}} \approx 0. \quad (8)$$

By eliminating  $\delta c_{\text{N}_2}$  in Eq. (7) using the relation expressed as Eq. (8), we obtain the following equation:

$$\text{PBE}/c_{\text{target}} = \Delta \varepsilon_{\text{O}_2} \delta c_{\text{O}_2} + \Delta \varepsilon_{\text{Ar}} \delta c_{\text{Ar}}, \quad (9)$$

where  $\Delta \varepsilon_{\text{O}_2}$  and  $\Delta \varepsilon_{\text{Ar}}$  are delta coefficients, defined as the difference between the pressure-broadening coefficient of O<sub>2</sub> or Ar from that of N<sub>2</sub>. Thus the delta coefficients can be estimated from the empirical relationship between PBEs and matrix gas variations. In the next section, we examine this empirical relationship in the context of CO<sub>2</sub> and CH<sub>4</sub> measurements obtained in a series of experiments.

### 3.1 Relationship between matrix gas composition and pressure-broadening effects

The effects of pressure broadening due to changes in the matrix gas composition on CO<sub>2</sub> and CH<sub>4</sub> measurements were examined using a dynamic gas blending unit (Fig. 1). The unit consists of two sets of high-pressure cylinders, thermal mass flow controllers, precise flow meters, and the three WS-CRDS instruments. In the experiments, compressed air and high-purity inert gas (< 99.9999 % N<sub>2</sub>, O<sub>2</sub>, or Ar, Japan Fine Products, Inc., Kanagawa, Japan) from these two high-pressure cylinders were dynamically mixed at a certain blending ratio by controlling their flow rates with the mass flow controllers (model 3660, Kofloc, Tokyo, Japan, for compressed air control; model SEC-E40, Horiba Stec, Tokyo, Japan, for pure inert gas control), which were calibrated precisely by means of the high-precision flow meters (mol-bloc/molbox flow calibration system, DH Instruments, Inc., Phoenix, AZ, USA). The mixed sample flow was supplied to the WS-CRDS instruments (models EnviroSense 3000i, G-1301, and G-2301) for quantification of the target gases. The mole fractions of the target gases were calculated as the average values observed over a period of 5 min with approximately 3 min intervals for sample stabilization after adjusting the blending ratio.

As mentioned above, the individual pure inert gases were obtained commercially; the compressed air was prepared in

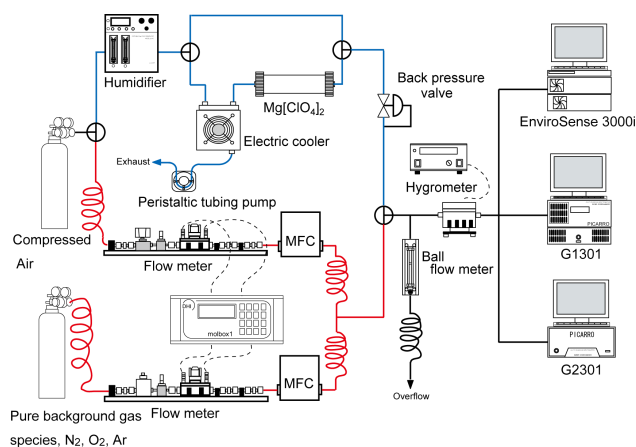


**Fig. 1.** Schematic diagram of the experimental system. The system consists of a sample humidification unit and a dynamic gas blending unit. Compressed air is supplied to the WS-CRDS instruments after adjustment of water vapor concentration via the humidification unit (blue line), while the mole fraction of the background gas in the sample air is adjusted through the dynamic gas blending unit (red line). See more detail in the text.

our laboratory using ambient air collected outside the laboratory. This ambient air was dehumidified by passing through a Nafion Permapure dryer (PD-200T-24, Perma Pure LLC, Toms River, NJ, USA) and a chemical trap packed with phosphorous pentoxide (P<sub>2</sub>O<sub>5</sub>, Sicapent<sup>®</sup>, EMD Millipore, Billerica, MA, USA). The dew point of the dehumidified ambient air was less than  $-80^{\circ}\text{C}$ . Calibrated by means of NDIR and gas chromatography/flame ionization detection with reference to the National Institute for Environmental Studies standard gas scale (Machida et al., 2008), the mole fractions of CO<sub>2</sub> and CH<sub>4</sub> in the compressed air were 402.26 ppm and 1917.57 ppb, respectively. Typical analytical precisions ( $\pm 1\sigma$ ) for CO<sub>2</sub> and CH<sub>4</sub> were 0.03 ppm and 1.7 ppb, respectively. The mole fraction of N<sub>2</sub> and O<sub>2</sub> in the compressed air was determined by measuring O<sub>2</sub>/N<sub>2</sub> ratio according to the method developed by Tohjima (2000). Here, we assume that mole fractions of Ar and other noble gases in the compressed air were identical to the reported annual average values at Hateruma in 2000 reported by Tohjima (2000). Uncertainty in the O<sub>2</sub> determination is approximately  $\pm 10$  ppm.

The magnitudes of PBEs due to changes in the matrix gas composition can be calculated as:

$$\text{PBE} = \Delta c - D, \quad (10)$$

where  $\Delta c$  and  $D$  indicate the observed variations in the mole fraction of the target gases and dilution effects on the target gases owing to the addition of the inert gases, respectively. The dilution effects in Eq. (10) were also calculated from the mole fractions of the target gases and the flow rates of the compressed air and pure inert gas:

$$D = c_0 \times \left( 1 - \frac{F_{\text{comp}}}{F_{\text{comp}} + F_{\text{inert}}} \right), \quad (11)$$

where  $c_0$  is the original mole fraction of the target gas before blending with the inert gas. The variables  $F_{\text{comp}}$  and  $F_{\text{inert}}$  indicate the flow rates of the compressed air and the inert gas, respectively. Using Eqs. (10) and (11), PBEs are calculated from following equation.

$$\text{PBE} = \Delta c - c_0 \times \left( 1 - \frac{F_{\text{comp}}}{F_{\text{comp}} + F_{\text{inert}}} \right). \quad (12)$$

We examined PBEs on CO<sub>2</sub> and CH<sub>4</sub> by increasing the mole fractions of N<sub>2</sub>, O<sub>2</sub>, and Ar in the sample air from their natural levels to 2.5, 8.8, and 27.7 %, respectively. A linear behavior in PBEs for both CO<sub>2</sub> (Fig. 2) and CH<sub>4</sub> (Fig. 3) was observed with increasing inert gas mole fraction in the sample air within the investigated range for the three WS-CRDS instruments; the linear behavior depended on the inert gas species. For example, N<sub>2</sub> addition resulted in an apparent decrease of CO<sub>2</sub>, whereas O<sub>2</sub> and Ar addition resulted in an apparent increase of CO<sub>2</sub>. For a 2.5 % increase of N<sub>2</sub>, O<sub>2</sub>, and Ar, G-1301 showed apparent CO<sub>2</sub> and CH<sub>4</sub> variations of  $-0.93$ ,  $+0.23$ , and  $+0.01$  ppm and  $-1.08$ ,  $+0.22$ , and  $+0.02$  ppb, respectively. These results suggest that PBEs generated by these inert gases are expressed as linear functions with respect to variations of the matrix gas composition for both CO<sub>2</sub> and CH<sub>4</sub>. Furthermore, the apparent variations of CO<sub>2</sub> and CH<sub>4</sub> indicate that N<sub>2</sub> imparts the greatest PBEs followed by O<sub>2</sub>, whereas Ar imparts the smallest PBEs.

Nakamichi et al. (2006) investigated PBEs of pure inert gases, including N<sub>2</sub>, O<sub>2</sub>, and Ar, for rotational transitions in the  $(3\ 0^0\ 1)_{\text{III}} \leftarrow (0\ 0\ 0)$  band of CO<sub>2</sub> at around 1600 nm within the temperature range 263–326 K. They observed a linear PBEs response with increasing inert gas, and the obtained pressure-broadening coefficients decreased in the order N<sub>2</sub> < O<sub>2</sub> < Ar. For example, the pressure-broadening coefficient (unit:  $\gamma\ \text{cm}^{-1}\ \text{atm}^{-1}$ ) for CO<sub>2</sub> at 298 K was 0.078 for N<sub>2</sub>, 0.067 for O<sub>2</sub>, and 0.062 for Ar (Nakamichi et al., 2006). Our experimental results agree reasonably well with those published results.

From our results, we calculated the delta coefficients for CO<sub>2</sub> and CH<sub>4</sub> according to Eq. (9) by a linear least squares analysis (Table 1). Although different delta coefficients were obtained among the WS-CRDS instruments, no significant differences were found in the PBEs calculations among these instruments in the present work. Hereafter we focus on the results from G-1301 as a representative case.

### 3.2 Impacts of pressure-broadening effects on the WS-CRDS measurements

In this section, we discuss possible impacts of PBEs on the WS-CRDS measurements using the estimated delta coefficients. As an example, we estimated the PBEs for CO<sub>2</sub> at

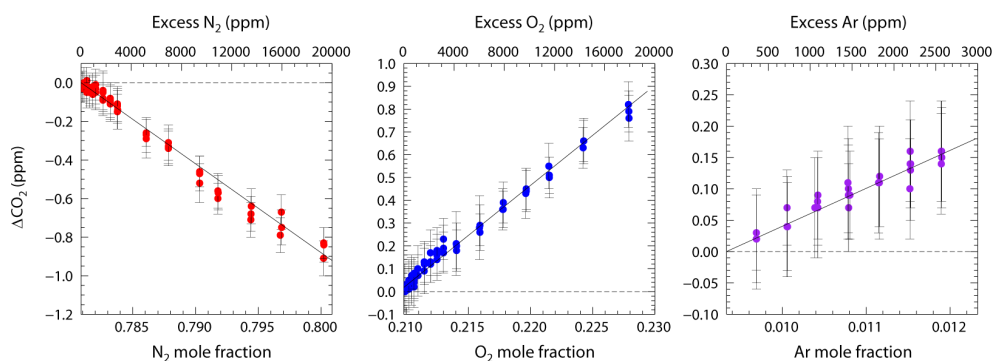


**Fig. 2.** Relationship between excess mole fraction of inert gases relative to their ambient levels and the resulting pressure-broadening effects on CO<sub>2</sub> measurements for WS-CRDS model G-1301. For each plot, the bottom axis indicates the increase in the amount of added inert gas in the sample air relative to the gas's ambient level, and the top axis indicates the relative increase in inert gas with respect to the bottom axis. The vertical bars in each plot denote the standard deviation ( $\pm 1\sigma$ ) determined from the precision of WS-CRDS measurements and the flow meter. Errors in the calculation of N<sub>2</sub>, O<sub>2</sub>, and Ar mole fraction are less than 74, 75, and 19 ppm, respectively. The solid line is the relationship between the changes in matrix gas composition resulting from the inert gas addition and pressure-broadening effects, as calculated by linear least squares analysis.

**Table 1.** Calculated difference of pressure-broadening coefficients for O<sub>2</sub> and Ar from the coefficient of N<sub>2</sub> for CO<sub>2</sub> and CH<sub>4</sub>\*

Model	Inert gas	Delta coefficient ( $\Delta\epsilon$ )	
		CO <sub>2</sub> $\times 10^{-7}$	CH <sub>4</sub> $\times 10^{-8}$
EnviroSense 3000i	O <sub>2</sub>	1.18 (0.01)	2.77 (0.06)
	Ar	2.10 (0.11)	5.67 (0.55)
G-1301	O <sub>2</sub>	1.13 (0.01)	2.62 (0.06)
	Ar	1.82 (0.07)	6.44 (0.48)
G-2301	O <sub>2</sub>	1.14 (0.01)	2.36 (0.07)
	Ar	1.88 (0.08)	5.67 (0.55)

\* Numbers in parentheses are standard errors of the corresponding delta coefficients estimated by the linear least squares analysis.

400 ppm and for CH<sub>4</sub> at 2000 ppb in response to O<sub>2</sub> and Ar variations for G-1301 (Fig. 4). Here we calculated PBEs from  $-20\,000$  to  $+20\,000$  ppm relative to the ambient O<sub>2</sub> level and from zero to  $+7000$  ppm relative to the ambient Ar level. The estimated PBEs corresponded to variations in target gas measurements from about  $-1.6$  to  $+1.5$  ppm for CO<sub>2</sub> and from  $-2.3$  to  $+2.0$  ppb for CH<sub>4</sub>.

Chen et al. (2010) reported that compositions of background gases (N<sub>2</sub>, O<sub>2</sub>, Ar) in synthetic standard gases can significantly differ from those in natural ambient air while natural variations of these gases in the well-mixed atmosphere may have negligible impact on the WS-CRDS measurements. Past studies revealed that atmospheric oxygen shows clear seasonal and interannual variability, whereas variation in the mole fraction of atmospheric argon is negligible (Keeling et al., 2004; Tohjima et al., 2005). Due to consumption by fossil fuel combustion, land biotic photosynthesis and aspiration, and the sea-air gas exchange,

oxygen generally shows summertime maximum and wintertime minimum with seasonal amplitude less than 200 ppm, and long-term decreasing rate of approximately  $4\text{ ppm yr}^{-1}$  (e.g. Keeling and Shertz, 1992). Based on the observed oxygen variations, we estimated the impacts of oxygen variation within  $\pm 200$  ppm relative to atmospheric composition on the WS-CRDS measurements. The calculated PBEs are approximately  $\pm 0.01$  ppm for CO<sub>2</sub> and  $\pm 0.01$  ppb for CH<sub>4</sub>, respectively. These results indicate that the oxygen natural variations have marginal impact on the WS-CRDS measurements.

The impacts of PBEs due to the difference of background gas composition in synthetic standard gases can be inferred through the measurements of a synthetic standard gas produced by Japan Fine Products. According to Japan Fine Products, the relative error for the O<sub>2</sub> and Ar mole fractions in N<sub>2</sub>-balanced N<sub>2</sub>/O<sub>2</sub>/Ar synthetic air is guaranteed within  $\pm 5\%$  from the nominal atmospheric O<sub>2</sub> and Ar mole fractions, and the O<sub>2</sub> mole fraction is guaranteed within  $\pm 2\%$  for N<sub>2</sub>-balanced N<sub>2</sub>/O<sub>2</sub> synthetic air. On the basis of these production errors, we can restrict the PBEs from  $\pm 0.51$  ppm for CO<sub>2</sub> and from  $-0.69$  to  $+0.57$  ppb for CH<sub>4</sub> for our measurements of standard gases diluted with the N<sub>2</sub>/O<sub>2</sub>/Ar synthetic air. On the other hand, PBEs for the standard gas with N<sub>2</sub>/O<sub>2</sub> synthetic air are restricted to be from about  $-0.50$  to  $-0.87$  ppm for CO<sub>2</sub> and from  $-1.4$  to  $-1.0$  ppb for CH<sub>4</sub>.

To prevent possible PBEs derived from variations in matrix gas composition, purified air is the preferred balance gas to be used for gas standards for WS-CRDS, because purified air is expected to have the same background gas composition of N<sub>2</sub>, O<sub>2</sub>, and Ar as that found in ambient air. Japan Fine Products uses ambient air to produce purified air, in which H<sub>2</sub>O and atmospheric trace gases are removed by cryogenic separation. After the cryogenic separation, any remaining impurities in the processed air are removed by passing the air

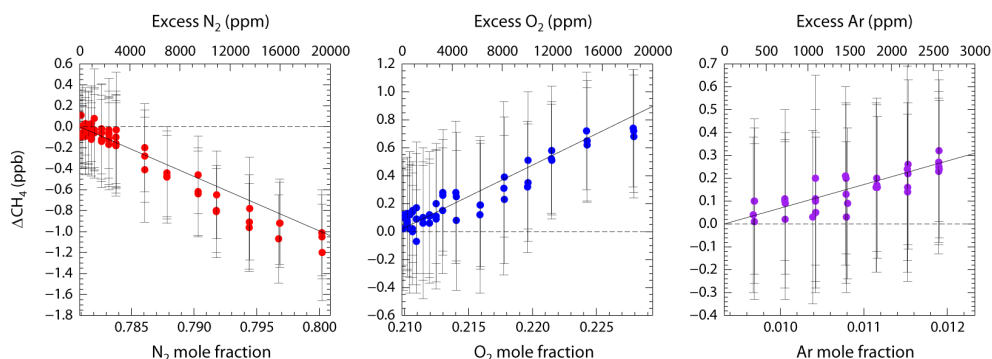


Fig. 3. The same as Fig. 2, but for CH<sub>4</sub>.

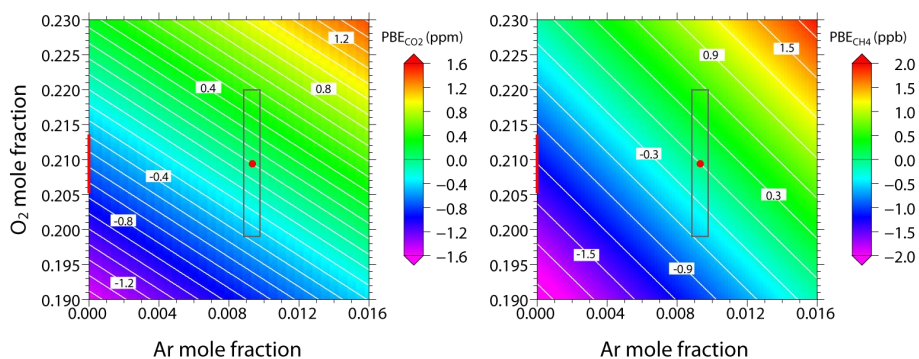


Fig. 4. Estimated pressure-broadening effects resulting from variations in matrix gas composition as a function of O<sub>2</sub> and Ar mole fraction for CO<sub>2</sub> measurements at 400 ppm (left) and for CH<sub>4</sub> measurements at 2000 ppb (right). The red circles denote ambient levels of O<sub>2</sub> and Ar. The gray solid rectangle denotes the  $\pm 5\%$  range of O<sub>2</sub> and Ar relative to their ambient levels. The thick red line on the y-axis indicates O<sub>2</sub> variation within  $\pm 2\%$  from its ambient level. The error associated with these estimations is negligible (less than 1% of the estimated values).

through columns packed with a heated Pt catalyst and molecular sieves (Tohjima et al., 2008). During these purification processes, O<sub>2</sub> can be removed from the processed air due to the oxidation of organic compounds and to strong absorption onto the molecular sieves when the sieves are in fresh condition, although N<sub>2</sub> and Ar are not absorbed at significant levels by the sieves. We have often checked the O<sub>2</sub> mole fraction in purified air from Japan Fine Products by means of N<sub>2</sub>/O<sub>2</sub> ratio analysis (Tohjima et al., 2008), which has revealed that O<sub>2</sub> decreases from ambient levels empirically by 1000 ppm, at most. In this case, the PBEs derived from the O<sub>2</sub> decrease are estimated to be up to  $-0.05$  ppm for CO<sub>2</sub> and  $-0.05$  ppb for CH<sub>4</sub> (typically the O<sub>2</sub> decrease is less than 500 ppm, corresponding to  $-0.02$  ppm for CO<sub>2</sub> and  $-0.03$  ppb for CH<sub>4</sub>), which would be only a marginal impact.

From these results, we recommend implementation of purified or natural ambient air-based standard gases for the calibration of WS-CRDS. In our laboratory, we have prepared a series of standard gases with different CO<sub>2</sub> and CH<sub>4</sub> mole fraction individually from natural ambient air (typically 400 ppm for CO<sub>2</sub>, 2000 ppb for CH<sub>4</sub>). The standard gases are prepared by diluting the natural ambient air with the purified

air (lower standard: ca. 380 ppm for CO<sub>2</sub>, 1800 ppb for CH<sub>4</sub>) and by adding pure synthetic CO<sub>2</sub> and CH<sub>4</sub> (higher standard: ca. 420 ppm for CO<sub>2</sub>, 2200 for CH<sub>4</sub>). During the air compression process, the oxygen mole fraction in these standard gases will slightly decrease from the original natural mole fraction by a few tens of ppm due to dissolution into the condensed water pool generated by cryogenic dehumidification in our air compression system and dilution by the addition of the purified air and pure CO<sub>2</sub> and CH<sub>4</sub>. However, such decrease has negligible impact on the magnitude of PBEs as well as isotopic bias (see next section in detail) resulting from the addition of pure synthetic CO<sub>2</sub> and CH<sub>4</sub>.

#### 4 Isotope correction for CO<sub>2</sub> measurements

As was reported by Chen et al. (2010), WS-CRDS measurements are biased due to the difference in the fractional abundance of each isotopologue of a target gas between the calibration gas and air sample: WS-CRDS determines the mole fraction of a target gas by evaluating only the main isotopologue of the target gas (e.g. <sup>12</sup>C<sup>16</sup>O<sup>16</sup>O for CO<sub>2</sub> measurements) in the air sample, under the assumption that the

fractional abundances of minor isotopologues in the air sample are the same as those in the calibration gas.

The fractional abundance of each isotopologue can be calculated from stable isotopic analysis. Since variation in the stable isotope abundance of a specific element is usually very small, the isotope abundance is expressed as a deviation from a defined standard material in permil (‰) using delta notation. For example, stable carbon isotope ratio is defined as follows:

$$\delta^{13}\text{C} (\text{‰}) = \left[ \frac{{}^{13}R_{\text{sam}}}{{}^{13}R_{\text{ref}}} - 1 \right] \times 1000, \quad (13)$$

where  ${}^{13}R_{\text{sam}}$  and  ${}^{13}R_{\text{ref}}$  is absolute ratio of  ${}^{13}\text{C}$  and  ${}^{12}\text{C}$  abundance  ${}^{13}\text{C}/{}^{12}\text{C}$  for a sample and a reference material, respectively. Similarly, stable oxygen isotope ratio is defined as

$$\delta^{18}\text{O} (\text{‰}) = \left[ \frac{{}^{18}R_{\text{sam}}}{{}^{18}R_{\text{ref}}} - 1 \right] \times 1000. \quad (14)$$

For stable carbon and oxygen isotopic analysis, Vienna Pee Dee Belemnite (VPDB) and Vienna Standard Mean Ocean Water (VSMOW) are referenced as standard materials.

Chen et al. (2010) derived an isotopic correction equation for CO<sub>2</sub> measurements by WS-CRDS instrument due to the difference of  $\delta^{13}\text{C}$  and  $\delta^{18}\text{O}$  values of CO<sub>2</sub> in ambient air ( $\delta^{13}\text{C}_{\text{amb}}$ ,  $\delta^{18}\text{O}_{\text{amb}}$ ) from those in synthetic standard gas ( $\delta^{13}\text{C}_{\text{syn}}$ ,  $\delta^{18}\text{O}_{\text{syn}}$ ) according to following equation:

$$\text{CO}_{2\text{amb}} = \text{CO}_{2\text{CRDS}} \times \left[ \frac{1 + {}^{13}R_{\text{ref}} \times (1 + \delta^{13}\text{C}_{\text{amb}}) + 2 \times {}^{18}R_{\text{ref}} \times (1 + \delta^{18}\text{O}_{\text{amb}})}{1 + {}^{13}R_{\text{ref}} \times (1 + \delta^{13}\text{C}_{\text{syn}}) + 2 \times {}^{18}R_{\text{ref}} \times (1 + \delta^{18}\text{O}_{\text{syn}})} \right], \quad (15)$$

where  $\text{CO}_{2\text{amb}}$  and  $\text{CO}_{2\text{CRDS}}$  are the CO<sub>2</sub> mole fraction in ambient air and the CO<sub>2</sub> value determined by WS-CRDS, respectively. The researchers calculated the isotopic biases based on reported  $\delta^{13}\text{C}$  and  $\delta^{18}\text{O}$  values typically found for CO<sub>2</sub> in synthetic standard gases ( $\delta^{13}\text{C} = -37 \pm 11$  ‰ vs. VPDB, and  $\delta^{18}\text{O} = 24 \pm 10$  ‰ vs. VSMOW) (Coplen et al., 2002) and background atmosphere ( $\delta^{13}\text{C} = -8$  ‰ vs. VPDB,  $\delta^{18}\text{O} = 42$  ‰ vs. VSMOW) (GLOBALVIEW-CO2C13, 2009; Allison and Francey, 2007). The resulting calculated biases ranged from 0.14 to  $0.16 \pm 0.06$  ppm.

Although isotopic correction for CH<sub>4</sub> was not reported by Chen et al. (2010), we roughly calculated the correction value by referencing past studies. Here stable hydrogen isotope ratio ( $\delta D$ ) is defined as similar to that of carbon and oxygen:

$$\delta D (\text{‰}) = \left[ \frac{{}^2R_{\text{sam}}}{{}^2R_{\text{ref}}} - 1 \right] \times 1000, \quad (16)$$

where  ${}^2R_{\text{sam}}$  and  ${}^2R_{\text{ref}}$  is  $D/H$  ratio for a sample and reference material. The  $\delta D$  value is also normalized to the

VSMOW scale. For the methane measurements, isotopic correction equation is given as:

$$\text{CH}_{4\text{amb}} = \text{CH}_{4\text{CRDS}} \times \left[ \frac{1 + {}^{13}R_{\text{ref}} \times (1 + \delta^{13}\text{C}_{\text{amb}}) + 4 \times {}^2R_{\text{ref}} \times (1 + \delta D_{\text{amb}})}{1 + {}^{13}R_{\text{ref}} \times (1 + \delta^{13}\text{C}_{\text{syn}}) + 4 \times {}^2R_{\text{ref}} \times (1 + \delta D_{\text{syn}})} \right]. \quad (17)$$

If we assume that typical  $\delta^{13}\text{C}$  and  $\delta D$  values of synthetic CH<sub>4</sub> are close to those for fossil fuel production of  $-40 \pm 7$  ‰ for  $\delta^{13}\text{C}$  (VPDB) and  $-175 \pm 10$  ‰ for  $\delta D$  (VSMOW) (Snover et al., 2000), and if we use  $\delta^{13}\text{C}$  and  $\delta D$  values for ambient CH<sub>4</sub> in northern hemispheric pristine air of  $-47.4 \pm 0.1$  ‰ for  $\delta^{13}\text{C}$  (VPDB) and  $-91 \pm 5$  ‰ for  $\delta D$  (VSMOW) (Quay et al., 1999), the correction value is estimated according to Eq. (17) to be about  $0.06\text{--}0.07 \pm 0.3$  ppb depending on the mixing ratios of CH<sub>4</sub>. Taking into account the typical analytical precision of a WS-CRDS instrument ( $\pm 0.3$  ppb), this result indicates that the isotopic bias for CH<sub>4</sub> measurements is not significant. We therefore examined the correction value only for CO<sub>2</sub> measurements.

We assessed the CO<sub>2</sub> isotopic correction method through comparison between the experimentally determined isotopic biases and theoretically calculated isotopic collection values according to Eq. (15). The isotopic biases were estimated from the difference in CO<sub>2</sub> measurements between WS-CRDS and NDIR. For this comparison, we prepared three CO<sub>2</sub>-in-air high-pressure cylinders as sample gases and six high-pressure cylinders for instrumental calibration. The three sample cylinders consisted of compressed natural air and a mixture of pure CO<sub>2</sub>, having different mole fractions and stable isotope ratios, and purified air. The mole fraction and stable carbon and oxygen isotope ratios of CO<sub>2</sub> in these sample cylinders are listed in Table 2. For the calibration gas, each high-pressure cylinder contained a different CO<sub>2</sub> mole fraction (350.35, 359.89, 370.22, 389.04, 419.78, or 429.59 ppm) with similar stable isotope ratios ( $\delta^{13}\text{C} = -29.64 \pm 0.22$  ‰ vs. VPDB,  $\delta^{18}\text{O} = -27.53 \pm 1.09$  ‰ vs. VPDB). Following the method of Tohjima et al. (2009), isotopic biases for the NDIR measurements were corrected precisely using the same NDIR instrument after the determination of stable carbon and oxygen isotope ratios by a conventional isotope ratio mass spectrometer (Finnigan MAT 252, ThermoQuest, Bremen, Germany) with dual inlets. PBEs for the WS-CRDS measurements were also corrected using our experimental results, while the background gas composition was determined according to the method reported by Tohjima (2000).

As an example, the CO<sub>2</sub> mole fractions, isotopic values, and their correction values from NDIR and the WS-CRDS instrument (G-1301) for three standard gas samples are summarized in Table 2, along with theoretically calculated isotopic correction values. The experimentally determined isotopic biases agreed well with the calculated correction values within the experimental errors, suggesting no significant differences between these two methods. From these results, we have demonstrated that isotopic biases for CO<sub>2</sub>

**Table 2.** Comparison of experimental and theoretical isotopic correction values\*.

Sample gas	NDIR	$\delta^{13}\text{C}/\delta^{18}\text{O}$ (‰)		Isotopic correction for NDIR**	WS-CRDS	PBE correction for WS-CRDS***	Experimental isotopic correction value (NDIR – WS-CRDS)	Calculated isotopic correction value	Experimental – theoretical
Compressed ambient air	402.15 ± 0.02	-9.07 ± 0.01	-2.29 ± 0.02	+0.11	402.12 ± 0.04	+0.01	0.13 ± 0.04	0.13 ± 0.07	0 ± 0.08
Synthetic STD 1	383.23 ± 0.01	-28.69 ± 0.01	-27.39 ± 0.02	+0.01	383.23 ± 0.05	+0.02	-0.01 ± 0.05	0 ± 0.07	-0.01 ± 0.08
Synthetic STD 2	369.79 ± 0.01	57.09 ± 0.02	-28.46 ± 0.02	+0.36	369.73 ± 0.04	+0.04	0.38 ± 0.04	0.35 ± 0.07	0.03 ± 0.08

\* Values for CO<sub>2</sub> mole fraction are given in ppm. \*\* The correction values were calculated according to the method reported by Tohjima et al. (2009). \*\*\* The correction values were calculated on the basis of our results (see Sect. 3.2). The background gas composition was determined by Tohjima et al. (2000).

measurements can be corrected according to the method by Chen et al. (2010) using isotopic values of CO<sub>2</sub>.

## 5 Water correction functions for three different WS-CRDS models

We determined the water correction functions for the three WS-CRDS instruments under the same experimental conditions using the above-mentioned humidification system (Fig. 1). In this experiment, we used the same compressed ambient air prepared for the gas blending experiments (see Sect. 3.1). The compressed air was introduced into the WS-CRDS instruments through a dew point generator (model LI-610, Li-Cor, Inc., Lincoln, NE, USA) for sample humidification while the excess flow was exhausted through the chilled mirror dew point hygrometer (model DPH-503H, Tokyo Opto-Electronics Co., Ltd.) to check the absolute water vapor concentration. In this experiment, the humidifier was slightly modified. The compressed air was split into two flows with and without passing through the built-in condenser. The sample flow, which bypasses the condenser, converges with the humidified sample flow from the condenser through a needle valve. The bypassed flow was activated when making the sample air with water vapor concentration below 0.5%. The water vapor concentration was adjusted using the needle valve. The humidified air sample was supplied to the WS-CRDS instruments for 5 min with and without passing through a two-step dehumidification unit, which consisted of an electric cooler (thermoelectric dehumidifier, DH-109, Komatsu Electronics Inc., Kanagawa, Japan) and a chemical trap filled with magnesium perchlorate (20/48 mesh, Wako Pure Chemical Industries, Osaka, Japan), making the dew point of the humid air sample less than -50 °C. We used a back pressure valve (model 6800, Kofloc, Tokyo, Japan) downstream of the sample humidification unit in order to prevent potential influence of magnesium perchlorate on CO<sub>2</sub> mixing ratios due to pressure fluctuation during the valve switching (Chen et al., 2010). To correct CO<sub>2</sub> drifts due to changes in the solubility of CO<sub>2</sub> in the water pool of the humidifier, dry or humidified air was supplied to the WS-CRDS instruments alternately as reported by past studies (Chen et al., 2010); no significant variations in the solubility of CH<sub>4</sub> were observed.

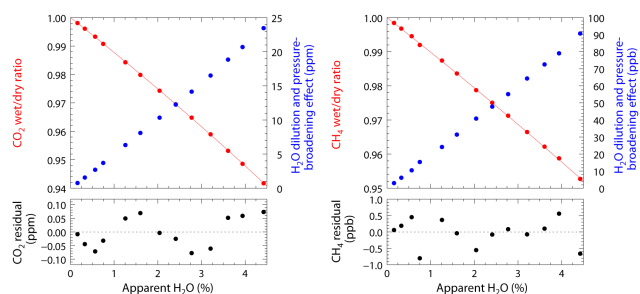


**Fig. 5.** The response of CO<sub>2</sub> and CH<sub>4</sub> against apparent water vapor concentration (values obtained from WS-CRDS measurements (model G-1301)) along with the residuals from the fitting functions. The wet/dry ratio (left y-axis) indicates the ratio of the measured mixing ratio of the target gases in the wet and dry sample air, and the corresponding water vapor dilution and pressure-broadening effects (right y-axis) are defined as the difference between the dry and wet mixing ratios of the target gases. The solid red lines are fitting curves for the wet/dry ratios with parameters listed in Table 3.

We examined the WS-CRDS response for CO<sub>2</sub> and CH<sub>4</sub> at water vapor concentrations of approximately 0.16 to 4.4% (Fig. 5). In the water vapor range examined here, the wet to dry ratio (wet/dry) of the target gas mixing ratio decreased to about 0.94 for CO<sub>2</sub> and 0.95 for CH<sub>4</sub>, corresponding to a decrease of 25 ppm and 95 ppb, respectively. The water correction function was determined from the relationship between the WS-CRDS reading of the water vapor concentrations and the wet/dry ratios for CO<sub>2</sub> and CH<sub>4</sub> by second-order polynomial fitting in order to correct the impact of self-broadening effect of water vapor itself (Chen et al., 2010):

$$\frac{X_{\text{wet}}}{X_{\text{dry}}} = 1 - a \cdot [\text{H}_2\text{O}]_{\text{CRDS}} - b \cdot [\text{H}_2\text{O}]_{\text{CRDS}}^2, \quad (18)$$

where  $[\text{H}_2\text{O}]_{\text{CRDS}}$  indicates water vapor concentration reported by the WS-CRDS instrument. Estimated linear (a) and quadratic (b) terms in Eq. (18) are listed in Table 3. The residuals from the fitting curve were within ± 0.08 ppm and ± 0.8 ppb for CO<sub>2</sub> and CH<sub>4</sub>, respectively (Fig. 5). All the coefficients of determination ( $R^2$ ) for both CO<sub>2</sub> and CH<sub>4</sub> from individual WS-CRDS instruments were greater than 0.999.

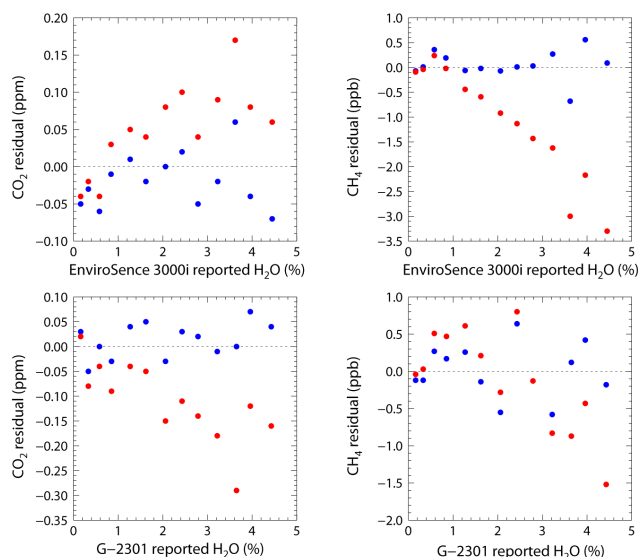
Chen et al. (2010) showed that water correction function is transferable between WS-CRDS instruments (model

**Table 3.** Water correction functions for three different WS-CRDS instruments along with the correction functions from past studies.

Group	Instrument model	CO <sub>2</sub> : linear (10 <sup>-2</sup> )/quadratic (10 <sup>-4</sup> ) terms	CH <sub>4</sub> : linear (10 <sup>-2</sup> )/quadratic (10 <sup>-4</sup> ) terms	Water vapor range (%)
Chen et al. (2010)	G-1301	1.20/2.67	0.98/2.39	0.6–6
Winderlich et al. (2010)	EnviroSense 3000i	1.205 ± 0.002/2.03 ± 0.08	1.007 ± 0.005/1.45 ± 0.18	0–4
This study	EnviroSense 3000i	1.207 ± 0.004/2.4 ± 0.1	0.999 ± 0.007/2.1 ± 0.2	0.16–4.4
	G-1301	1.204 ± 0.007/2.5 ± 0.2	0.999 ± 0.013/1.4 ± 0.4	
	G-2301	1.216 ± 0.009/1.6 ± 0.3	0.968 ± 0.008/2.3 ± 0.2	

G-1301-m and G-1301) where the water vapor measurements of the G-1301 were corrected to those of G-1301-m. Based on our experiments, we evaluated the transferability of the determined water correction function among three WS-CRDS instruments. The water vapor measurements of EnviroSense 3000i and G-2301 was corrected to that of G-1301 with linear correlation, and then the water vapor correction function from G-1301 was applied to the experimental results from EnviroSense 3000i and G-2301 (Fig. 6). The residual errors of applied G-1301 water correction function shows substantially large value for both EnviroSense 3000i and G-2301 with increasing water vapor concentration, while the residuals of instrument-specific water correction functions are comparable to that of G-1301 (Fig. 5). Presumably, this incompatibility of the water correction function would indicate experimental bias likely due to CO<sub>2</sub> drift corrections resulting from the temperature-dependent variation in CO<sub>2</sub> dissolution in the water pool, although it might suggest the difference of instrument-specific water correction function among the WS-CRDS instruments. More precise experiments are needed to scrutinize the transferability of the water correction function.

Dehumidification of sample air would be a reliable method to reduce the uncertainty associated with the water correction of CO<sub>2</sub> and CH<sub>4</sub> measurements. We compared water correction values calculated from the water correction functions listed in Table 3 against reported water concentration along with previously reported water correction functions (Fig. 7). Although the CO<sub>2</sub> deviation for EnviroSense 3000i and Chen et al. (2010) is very small, the CO<sub>2</sub> and CH<sub>4</sub> deviations generally become large with increase of reported water vapor concentration, likely due to the difference of water vapor measurement scale among these instruments and uncertainties of the water correction functions. However, at lower water vapor concentrations, the deviation for all water correction functions agrees within the typical analytical precision ( $\pm 0.03$  ppm for CO<sub>2</sub>,  $\pm 0.3$  ppb for CH<sub>4</sub>) at reported water vapor concentrations of  $> 0.7\%$  for CO<sub>2</sub> and  $> 0.6\%$  for CH<sub>4</sub>. These results give an indication of sample dehumidification level to remove possible uncertainty associated with the water vapor correction. Taking into account laborious and delicate experiments for the determination of water correction function, potential temporal change of the water correction coefficients and the difference of these coefficients

**Fig. 6.** Transferability of water correction function from G-1301 among EnviroSense 3000i and G-2301. Residuals of CO<sub>2</sub> and CH<sub>4</sub> from instrument-specific and G-1301 water correction curve for EnviroSense 3000i and G-2301 are plotted as blue and red plots, respectively against reported water vapor concentration. Residuals from the water correction curve for G-1301 are calculated after the reported water vapor concentrations are collected to that of G-1301 scale with linear correlation.

between WS-CRDS instruments, we conclude that complete dehumidification or moderate dehumidification followed by application of a water correction function is the best strategy to remove uncertainty associated with water correction.

## 6 Conclusions

We investigated factors affecting WS-CRDS measurement, including effects from pressure broadening of the background gases' spectral lines, variations in isotopologues of the target gases, and dilution and pressure broadening of water vapor. Using a dynamic gas blending system, we determined the delta coefficients, defined as the difference in the pressure-broadening coefficients of O<sub>2</sub> and Ar from the coefficient of N<sub>2</sub>, by linear least squares analysis, and then calculated the magnitude of PBEs as a function of O<sub>2</sub> and Ar

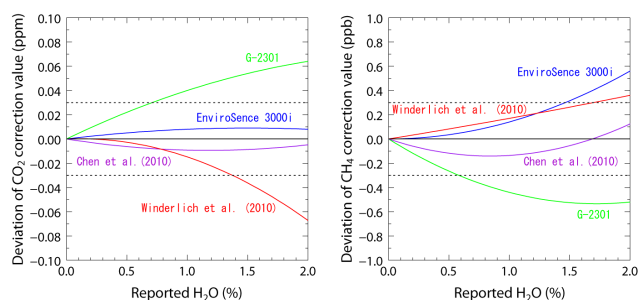


**Fig. 7.** Comparison of water correction functions for CO<sub>2</sub> and CH<sub>4</sub>. The solid lines indicate difference in calculated water correction values for the individual instrument-specific water correction function from those of G-1301 as a function of reported water vapor concentration. Blue: EnviroSense 3000i; green: G-2301; purple: G-1301-m from Chen et al. (2010); red: EnviroSense 3000i from Winderlich et al. (2010). The dashed lines indicate typical analytical precision of WS-CRDS instrument ( $\pm 0.03$  ppm for CO<sub>2</sub>,  $\pm 0.3$  ppb for CH<sub>4</sub>).

mole fraction. Our PBEs calculation showed that impact of natural variation of O<sub>2</sub> is negligible on the CO<sub>2</sub> and CH<sub>4</sub> measurements. In contrast, significant PBEs were inferred for the measurement of synthetic standard gases. The magnitudes of the PBEs were classified into three cases depending on the background gas. For the preparation of N<sub>2</sub>-balanced N<sub>2</sub>/O<sub>2</sub>/Ar and N<sub>2</sub>/O<sub>2</sub> synthetic air, the relative error for O<sub>2</sub> and Ar mole fraction is guaranteed  $\pm 5\%$  and  $\pm 2\%$  from their nominal composition. The corresponding PBEs impact on CO<sub>2</sub> and CH<sub>4</sub> were estimated to be up to about  $\pm 0.5$  ppm and  $\pm 0.7$  ppb for the former synthetic air, and from  $-0.49$  to  $-0.87$  ppm and from  $-1.4$  to  $-1.0$  ppb for the latter one, respectively. In contrast, the PBEs for purified air were estimated to be up to  $-0.05$  ppm for CO<sub>2</sub> and  $-0.01$  ppb for CH<sub>4</sub> on the basis of our O<sub>2</sub> analysis purified air. To ascertain the impact of variations in isotopologues on CO<sub>2</sub> measurements, we compared the isotopic bias between experimental values and theoretical calculations, whereas isotopic correction for CH<sub>4</sub> is estimated to be marginal. The isotopic bias from these two methods agreed well within the experimental error, suggesting that the isotopic bias can be corrected accurately by the theoretical calculation based on CO<sub>2</sub> stable isotope ratios. Using a sample humidification unit, we derived water correction functions for CO<sub>2</sub> and CH<sub>4</sub> from three different WS-CRDS instruments. Although the transferability of the correction functions among different WS-CRDS models was not proven, likely due to the experimental uncertainty, we observed no significant differences within the typical analytical precision in instrument-specific water correction values from the investigated instruments, nor within previously reported ones at water vapor concentrations  $> 0.7\%$  for CO<sub>2</sub> and  $> 0.6\%$  for CH<sub>4</sub>. These results suggest that complete dehumidification or moderate dehumidification followed by application of a water correction function is the best strategy

for obtaining highly accurate CO<sub>2</sub> and CH<sub>4</sub> measurements, along with calibration with natural air-based standard gases or purified air-balanced synthetic standard gases with the isotopic correction.

**Acknowledgements.** We thank T. Machida for his logistical support of our experiments. We are grateful to Y. Takahashi for CO<sub>2</sub> isotopic analysis. We also thank Y. Morino for valuable comments on our study. We gratefully acknowledge valuable comments from two reviewers to improve our manuscript. This study was conducted with financial support from the Ministry of the Environment, Japan as a Global Environment Research Account for National Institutes. Funding was also provided by the Global Environment Research Fund of the Ministry of the Environment, Japan (S-7-1).

Edited by: D. Griffith

## References

- Allison, C. E. and Francey, R. J.: Verifying Southern Hemisphere trends in atmospheric carbon dioxide stable isotopes, *J. Geophys. Res.*, 112, D21304, doi:10.1029/2006JD007345, 2007.
- Aydin, M., Verhulst, K. R., Saltzman, E. S., Battle, M. O., Monzka, S. A., Blake, D. R., Tang, Q., and Prather, M. J.: Recent decreases in fossil-fuel emissions of ethane and methane derived from firm air, *Nature*, 476, 198–202, doi:10.1038/nature10352, 2011.
- Baer, D. S., Paul, J. B., Gupta, M., and O’Keefe, A.: Sensitive absorption measurements in the near-infrared region using off-axis integrated-cavity-output spectroscopy, *Appl. Phys. B*, 75, 261–265, doi:10.1007/s00340-002-0971-z, 2002.
- Berden, G., Petters, R., and Meijer, G.: Cavity-enhanced absorption spectroscopy of the 1.5  $\mu\text{m}$  band system of jet-cooled ammonia, *Chem. Phys. Lett.*, 307, 131–138, 1999.
- Bischof, W.: The influence of the carrier gas on the infrared gas analysis of atmospheric CO<sub>2</sub>, *Tellus*, 27, 59–61, 1975.
- Brenninkmeijer, C. A. M., Crutzen, P., Boumard, F., Dauer, T., Dix, B., Ebinghaus, R., Filippi, D., Fischer, H., Franke, H., Frieß, U., Heintzenberg, J., Helleis, F., Hermann, M., Kock, H. H., Koepfel, C., Lelieveld, J., Leuenberger, M., Martinsson, B. G., Miemczyk, S., Moret, H. P., Nguyen, H. N., Nyfeler, P., Oram, D., O’Sullivan, D., Penkett, S., Platt, U., Pucek, M., Ramonet, M., Randa, B., Reichelt, M., Rhee, T. S., Rohwer, J., Rosenfeld, K., Scharffe, D., Schlager, H., Schumann, U., Slemr, F., Sprung, D., Stock, P., Thaler, R., Valentino, F., van Velthoven, P., Waibel, A., Wandel, A., Waschitschek, K., Wiedensohler, A., Xueref-Remy, I., Zahn, A., Zech, U., and Ziereis, H.: Civil Aircraft for the regular investigation of the atmosphere based on an instrumented container: The new CARIBIC system, *Atmos. Chem. Phys.*, 7, 4953–4976, doi:10.5194/acp-7-4953-2007, 2007.
- Buchwitz, M., de Beek, R., Burrows, J. P., Bovensmann, H., Warneke, T., Notholt, J., Meirink, J. F., Goede, A. P. H., Bergamaschi, P., Körner, S., Heimann, M., and Schulz, A.: Atmospheric methane and carbon dioxide from SCIAMACHY satellite data: initial comparison with chemistry and transport models, *Atmos. Chem. Phys.*, 5, 941–962, doi:10.5194/acp-5-941-2005, 2005.

- Chen, H., Winderlich, J., Gerbig, C., Hofer, A., Rella, C. W., Crosson, E. R., Van Pelt, A. D., Steinbach, J., Kolle, O., Beck, V., Daube, B. C., Gottlieb, E. W., Chow, V. Y., Santoni, G. W., and Wofsy, S. C.: High-accuracy continuous airborne measurements of greenhouse gases (CO<sub>2</sub> and CH<sub>4</sub>) using the cavity ring-down spectroscopy (CRDS) technique, *Atmos. Meas. Tech.*, 3, 375–386, doi:10.5194/amt-3-375-2010, 2010.
- Cunnold, D. M., Steele, L. P., Fraser, P. J., Simmonds, P. G., Prinn, R. G., Weiss, R. F., Porter, L. W., O'Doherty, S., Langenfelds, R. L., Krummel, P. B., Wang, H. J., Emmons, L., Tie, X. X., and Dlugokencky, E. J.: In situ measurements of atmospheric methane at GAGE/AGAGE sites during 1985–2000 and resulting source inferences, *J. Geophys. Res.*, 107, 4225, doi:10.1029/2001JD001226, 2002.
- Conway, T., Tans, P. P., Waterman, L. S., Thoning, K. W., Kitzis, D. R., Masarie, K. A., and Zhang, N.: Evidence for interannual variability of the carbon cycle from the National Oceanic and Atmospheric Administration/Climate Monitoring and Diagnostics Laboratory Global Air Sampling Network, *J. Geophys. Res.*, 99, 22831–22855, 1994.
- Coplen, T. B., Bohlke, J. K., De Bievre, P., Ding, T., Holden, N. E., Hopple, J. A., Krouse, H. R., Lamberty, A., Peiser, H. S., Revesz, K., Rieder, S. E., Rosman, K. J. R., Roth, E., Taylor, P. D. P., Vocke, R. D., and Xiao, Y. K.: Isotope-abundance variations of selected elements – (IUPAC Technical Report), *Pure Appl. Chem.*, 74, 1987–2017, 2002.
- Crosson, E. R.: A cavity ring-down analyzer for measuring atmospheric levels of methane, carbon dioxide, and water vapor, *Appl. Phys. B-Lasers O.*, 92, 403–408, 2008.
- Dlugokencky, E. J., Steele, L. P., Lang, P. M., and Masarie, K. A.: Atmospheric methane at Mauna Loa and Barrow observatories: Presentation and analysis of in situ measurements, *J. Geophys. Res.*, 100, 23103–23113, 1995.
- Dicke, R.: The effect of collisions upon the Doppler width of spectral lines, *Phys. Rev.*, 89, 472–473, 1953.
- Esler, M. B., Griffith, D. W. T., Wilson, S. R., and Steele, L. P.: Precision trace gas analysis by FT-IR spectroscopy. I. Simultaneous analysis of CO<sub>2</sub>, CH<sub>4</sub>, N<sub>2</sub>O, and CO in Air, *Anal. Chem.*, 72, 206–215, 2000.
- Galatry, L.: Simultaneous effect of Doppler and foreign gas broadening on spectral lines, *Phys. Rev.* 122, 1218–1223, 1961.
- GLOBALVIEW-CO2C13: Cooperative Atmospheric Data Integration Project – δ<sup>13</sup>C of Carbon Dioxide, CD-ROM, NOAA ESRL, Boulder, Colorado, also available via anonymous FTP to ftp.cmdl.noaa.gov, Path: ccc/co2c13/GLOBALVIEW (last access: 12 November 2012), 2009.
- Griffith, D. W. T.: Calculations of carrier gas effects in non-dispersive infrared analyzers I. Theory, *Tellus*, 34, 376–384, 1982.
- Griffith, D. W. T., Deutscher, N. M., Caldow, C. G. R., Kettlewell, G., Riggensbach, M., and Hammer, S.: A Fourier transform infrared trace gas analyser for atmospheric applications, *Atmos. Meas. Tech. Discuss.*, 5, 3717–3769, doi:10.5194/amtd-5-3717-2012, 2012.
- Griffith, D. W. T., Keeling, C. D., Adams, J. A., Guenther, P. R., and Bacastow, R. B.: Calculations of carrier gas effects in non-dispersive infrared analyzers. II. Comparisons with experiment, *Tellus*, 34, 385–397, 1982.
- Grutter, M.: Multi-gas analysis of ambient air using FTIR spectroscopy over Mexico city, *Atmósfera*, 16, 1–13, 2003.
- Hammer, S., Griffith, D. W. T., Konrad, G., Vardag, S., Caldow, C., and Levin, I.: Assessment of a multi-species in-situ FTIR for precise atmospheric greenhouse gas observations, *Atmos. Meas. Tech. Discuss.*, 5, 3645–3692, doi:10.5194/amtd-5-3645-2012, 2012.
- Kai, F. M., Tyler, S. C., Randerson, J. T., and Blake, D. R.: Reduced methane growth rate explained by decreased Northern Hemisphere microbial sources, *Nature*, 476, 194–197, doi:10.1038/nature10259, 2011.
- Keeling, C. D.: The concentration and isotopic abundances of carbon dioxide in the atmosphere, *Tellus*, 12, 200–203, 1960.
- Keeling, C. D., Whorf, T. P., Wahlen, M., and van der Plicht, J.: Interannual extremes in the rate of rise of atmospheric carbon dioxide since 1980, *Nature*, 375, 666–670, 1995.
- Keeling, R. F. and Shertz, S. R.: Seasonal and interannual variations in atmospheric oxygen and implications for the global carbon cycle, *Nature*, 358, 723–727, 1992.
- Keeling, R. F., Blaine, T., Paplawsky, B., Katz, L., Atwood, C., and Brockwell, T.: Measurement of changes in atmospheric Ar/N<sub>2</sub> ratio using a rapid-switching, single-capillary mass spectrometer system, *Tellus*, 56B, 322–338, 2004.
- Kozlova, E. A. and Manning, A. C.: Methodology and calibration for continuous measurements of biogeochemical trace gas and O<sub>2</sub> concentrations from a 300-m tall tower in central Siberia, *Atmos. Meas. Tech.*, 2, 205–220, doi:10.5194/amt-2-205-2009, 2009.
- Lowe, D. C., Guenther, P. R., and Keeling, C. D.: The concentration of atmospheric carbon dioxide at Baring Head, New Zealand, *Tellus*, 31, 58–67, 1979.
- Machida, T., Matsueda, H., Sawa, Y., Nakagawa, Y., Hirokuni, K., Kondo, N., Goto, K., Nakazawa, T., Ishikawa, K., and Ogawa, T.: Worldwide measurements of atmospheric CO<sub>2</sub> and other trace gas species using commercial airlines, *J. Atmos. Oceanic Technol.*, 25, 1744–1754, 2008.
- Marquis, M. and Tans, P.: Carbon Crucible, *Science*, 320, 460–461, 2008.
- Matsueda, H. and Inoue, H. Y.: Measurements of atmospheric CO<sub>2</sub> and CH<sub>4</sub> using a commercial airliner from 1993 to 1994, *Atmos. Environ.*, 30, 1647–1655, 1996.
- Messerschmidt, J., Geibel, M. C., Blumenstock, T., Chen, H., Deutscher, N. M., Engel, A., Feist, D. G., Gerbig, C., Gisi, M., Hase, F., Katrynski, K., Kolle, O., Lavric, J. V., Notholt, J., Palm, M., Ramonet, M., Rettinger, M., Schmidt, M., Sussmann, R., Toon, G. C., Truong, F., Warneke, T., Wennberg, P. O., Wunch, D., and Xueref-Remy, I.: Calibration of TCCON column-averaged CO<sub>2</sub>: the first aircraft campaign over European TCCON sites, *Atmos. Chem. Phys.*, 11, 10765–10777, doi:10.5194/acp-11-10765-2011, 2011.
- Montzka, S. A., Dlugokencky, E. J., and Butler, J. H.: Non-CO<sub>2</sub> greenhouse gases and climate change, *Nature*, 476, 43–50, doi:10.1038/nature10322, 2011.
- Nakamichi, S., Kawaguchi, Y., Fukuda, H., Enami, S., Hashimoto, Satoshi, Kawasaki, M., Umekawa, T., Morino, I., Suto, H., and Inoue, G.: Buffer-gas pressure broadening for the (3 0<sup>0</sup> 1)<sub>III</sub> ← (0 0 0) band of CO<sub>2</sub> measured with continuous-wave cavity ring-down spectroscopy, *Phys. Chem. Chem. Phys.*, 8, 364–368, 2006.

- O'Keefe, A.: Integrated cavity output analysis of ultra-weak absorption, *Chem. Phys. Lett.*, 293, 331–336, 1998.
- O'Keefe, A. and Deacon, A., G.: Cavity ring-down optical spectrometer for absorption measurements using pulsed laser sources, *Rev. Sci. Instrum.*, 59, 2544–2554, 1988.
- O'Keefe, A., Scherer, J. J., and Paul, J. B.: Integrated cavity output spectroscopy, *Chem. Phys. Lett.*, 307, 343–349, 1999.
- Paul, J. B., Lapson, L., and Anderson, J. G.: Ultrasensitive absorption spectroscopy with a high-finesse optical cavity and off-axis alignment, *Appl. Opt.*, 40, 4901–4910, 2001.
- Pearman, G. I. and Garratt, J. R.: Errors in atmospheric CO<sub>2</sub> concentration measurements arising from the use of reference gas mixtures different in composition to the sample air, *Tellus*, 27, 62–66, 1975.
- Prinn, R. G., Weiss, R. F., Fraser, P. J., Simmonds, P. G., Cunnold, D. M., Alyea, F. N., O'Doherty, S., Salameh, P., Miller, B. R., Huang, J., Wang, R. H. J., Hartley, D. E., Harth, C., Steele, L. P., Sturrock, G., Midgley, P. M., and McCulloch, A.: A history of chemically and radiatively important gases in air deduced from ALE/GAGE/AGAGE, *J. Geophys. Res.*, 105, 17751–17792, 2000.
- Quay, P. D., Stutsman, J., Wilbur, D., Snover, A., Dlugokencky, E., and Brown, T.: The isotopic composition of atmospheric methane, *Global Biogeochem. Cy.*, 13, 445–461, 1999.
- Richard, E. C., Kelly, K. K., Winkler, R. H., Wilson, R., Thompson, T. L., McLaughlin, R. J., Schmeltekopf, A. L., and Tuck, A. F.: A fast-response near-infrared tunable diode laser absorption spectrometer for in situ measurements of CH<sub>4</sub> in the upper troposphere and lower stratosphere, *Appl. Phys. B*75, 183–194, doi:10.1007/s00340-002-0935-3, 2002.
- Richardson, S. J., Miles, N. L., Davis, K. J., Crosson, E. R., Rella, C. W., and Andrews, A. E.: Field testing of cavity ring-down spectroscopy analyzers measuring carbon dioxide and water vapor, *J. Atmos. Oceanic Technol.*, 29, 397–406, 2012.
- Rigby, M., Prinn, R. G., Fraser, P. J., Simmonds, P. G., Langenfelds, R. L., Huang, J., Cunnold, D. M., Steele, L. P., Krummel, P. B., Weiss, R. F., O'Doherty, S., Salameh, P. K., Wang, H. J., Harth, C. M., Mühle, J., and Porter, L. W.: Renewed growth of atmospheric methane, *Geophys. Res. Lett.*, 35, L22805, doi:10.1029/2008GL036037, 2008.
- Saitoh, N., Imasu, R., Ota, Y., and Niwa, Y.: CO<sub>2</sub> retrieval algorithm for the thermal infrared spectra of the greenhouse gases observing satellite: Potential of retrieving CO<sub>2</sub> vertical profile from high-resolution FTS sensor, *J. Geophys. Res.*, 114, D17305, doi:10.1029/2008JD011500, 2009.
- Snover, A., Quay, P. D., and Hao, W. M.: The D/H content of methane emitted from biomass burning, *Global Biogeochem. Cy.*, 14, 11–24, 2000.
- Terao, Y., Mukai, H., Nojiri, Y., Machida, T., Tohjima, Y., Saeki, T., and Maksyutov, S.: Interannual variability and trends in atmospheric methane over the western Pacific from 1994 to 2010, *J. Geophys. Res.*, 116, D14303, doi:10.1029/2010JD015467, 2011.
- Tohjima, Y.: Method for measuring changes in the atmospheric O<sub>2</sub>/N<sub>2</sub> ratio by a gas chromatograph equipped with a thermal conductivity detector, *J. Geophys. Res.*, 105, 14575–14584, 2000.
- Tohjima, Y., Machida, T., Watai, T., Akama, I., Amari, T., and Moriwaki, Y.: Preparation of gravimetric standards for measurements of atmospheric oxygen and reevaluation of atmospheric oxygen concentration, *J. Geophys. Res.*, 110, D11302, doi:10.1029/2004JD005595, 2005.
- Tohjima, Y., Mukai, H., Nojiri, Y., Yamagishi, H., and Machida, T.: Atmospheric O<sub>2</sub>/N<sub>2</sub> measurements at two Japanese sites: estimation of global oceanic and land biotic carbon sinks and analysis of the variations in atmospheric potential oxygen (APO), *Tellus*, 60B, 213–225, 2008.
- Tohjima, Y., Katsumata, K., Morino, I., Mukai, H., Machida, T., Akama, I., Amari, T., and Tsunogai, U.: Theoretical and experimental evaluation of the isotope effect of NDIR analyzer on atmospheric CO<sub>2</sub> measurement, *J. Geophys. Res.*, 114, D13302, doi:10.1029/2009JD011734, 2009.
- Varghese, P. and Hanson, R.: Collisional narrowing effects on spectral line shapes measured at high resolution, *Appl. Opt.*, 23, 2376–2385, 1984.
- Winderlich, J., Chen, H., Höfer, A., Gerbig, C., Seifert, T., Kolle, O., Kaiser, C., Lavrič, J. V., and Heimann, M.: Continuous low-maintenance CO<sub>2</sub>/CH<sub>4</sub>/H<sub>2</sub>O measurements at the Zotino Tall Tower Observatory (ZOTTO) in Central Siberia, *Atmos. Meas. Tech. Discuss.*, 3, 1399–1437, doi:10.5194/amtd-3-1399-2010, 2010.
- Webster, C. R., May, R. D., Trimble, C. A., Chave, R. G., and Kendall, J.: Aircraft (ER-2) laser infrared absorption spectrometer (ALIAS) for *in-situ* stratospheric measurements of HCl, N<sub>2</sub>O, CH<sub>4</sub>, NO<sub>2</sub>, and HNO<sub>3</sub>, *Appl. Opt.*, 33, 454–472, 1994.
- Webster, C. R., Flesh, G. J., Scott, D. C., Swanson, J. E., May, R. D., Woodward, W. S., Gmachl, C., Capasso, F., Sivco, D. L., Baillargeon, J. N., Hutchinson, A. L., and Cho, A. Y.: Quantum-cascade laser measurements of stratospheric methane and nitrous oxide, *Appl. Opt.*, 40, 321–326, 2001.
- WMO: GAW Report No. 194 – 15th WMO/IAEA Meeting of Experts on Carbon Dioxide, Other Greenhouse Gases and Related Tracers Measurement Techniques, *Tech. Rep.*, World Meteorological Organization, 2009.
- Wunch, D., Toon, G. C., Blavier, J.-F., Washenfelder, R. A., Notholt, J., Connor, B. J., Griffith, D. W. T., Sherlock, V., and Wennberg, P. O.: The total carbon column observing network, *Phil. Trans. Roy. Soc. A*, 369, 2087–2112, doi:10.1098/rsta.2010.0240, 2012.
- Xiong, X., Barnett, C. D., Zhuang, Q., Machida, T., Sweeney, C., and Patra, P. K.: Mid-upper tropospheric methane in the high northern hemisphere: Spaceborne observations by AIRS, aircraft measurements, and model simulations, *J. Geophys. Res.*, 115, D19309, doi:10.1029/2009JD013796, 2010.
- Yokota, T., Yoshida, Y., Eguchi, N., Ota, Y., Tanaka, T., Watanabe, H., and Maksyutov, S.: Global concentrations of CO<sub>2</sub> and CH<sub>4</sub> retrieved from GOSAT: First preliminary results, *SOLA*, 5, 160–163, doi:10.2151/sola.2009-041, 2009.
- Yoshida, Y., Ota, Y., Eguchi, N., Kikuchi, N., Nobuta, K., Tran, H., Morino, I., and Yokota, T.: Retrieval algorithm for CO<sub>2</sub> and CH<sub>4</sub> column abundances from short-wavelength infrared spectral observations by the Greenhouse gases observing satellite, *Atmos. Meas. Tech.*, 4, 717–734, doi:10.5194/amt-4-717-2011, 2011.